1   **QUANTIFICATION OF SOLUBLE SOLIDS AND INDIVIDUAL SUGARS IN APPLES**

2   **BY RAMAN SPECTROSCOPY: A FEASIBILITY STUDY**

3   Olga Monago-Maraña[1,2], Nils Kristian Afseth[2], Svein Halvor Knutsen[2], Sileshi Gizachew

4   Wubshet[2], Jens Petter Wold[2]

5

6   [1]Department of Analytical Sciences, Faculty of Science, Avda. Esparta s/n, Crta. de Las Rozas-

7   Madrid, 28232, Las Rozas, Madrid, National Distance Education University (UNED), Spain

8

9   [2]Nofima AS – Norwegian Institute of Food, Fisheries and Aquaculture Research, Muninbakken

10   9-13, Breivika, Postboks 6122 Langnes, NO-9291 Tromsø, Norway

11

12   *corresponding author: olgamonago@ccia.uned.es; +34675673233

13

14   **Abstract**

15   This study reports the feasibility of using Raman spectroscopy for quantification of soluble solids and

16   individual sugars in apple. Six different commercial apple varieties were measured by Raman

17   spectroscopy at three different steps: 1) Intact apples with skin, 2) apples without skin and 3) juices

18   obtained from apples. Results indicated that it is possible to measure Raman signals to a depth of 8 mm

19   into the apple with a wide area Raman probe. Multivariate calibration models were established to

20   evaluate how well Raman spectra can be used to estimate the quality parameters SSC (%), total sugars,

21   glucose, fructose and sucrose. Estimation accuracy for SSC was comparable with what is achievable

22   with near-infrared spectroscopy: Root mean square error of cross-validation (RMSECV) = 0.66, 0.46

23   and 0.72 % and coefficients of determination (R^2) = 0.70, 0.85 and 0.63 for intact apples, apples without

24   skin and juices, respectively. Sucrose and glucose were well estimated with RMSECV of 2.8, 1.9, 2.1

25   mg/mL for glucose and 5.8, 3.9 and 3.7 mg/mL for sucrose, for the three sample cases, respectively.

26   Coefficient of determination was higher than 0.82 for all models. Regression coefficients for all

27   calibration models highlighted identifiable Raman bands that could be related to the target sugars.

28

29   **Keywords:** Raman spectroscopy; SSC; apples; non-destructive prediction; chemometrics; sugars.

30

31

32

33

34

35

1. Introduction

Apple is a widely produced and consumed fruit around the world. It is rich in sugar, vitamins, flavonoids, minerals and other nutrients attributed to health benefits. Sweetness is one of the most important components of fruit quality that determines the overall acceptability of apples (Harker et al., 2003; Janick et al., 1996). Sweetness is correlated to soluble solids content (SSC), which includes total solutes; e.g.; organic acids, amino acids, soluble pectins and has a major contribution from the sugars fructose, glucose and sucrose (Guan et al., 2015). SSC is an important parameter to determine flavour, ripeness as well as to predict optimal harvest time for apples. Refractometry of fruit juice is the standard method for SSC measurement, given as % or °Brix, unfortunately a destructive and rather time-consuming procedure. Quantification of individual sugars (fructose, glucose and sucrose) in apples are also of interest in connection with phenotyping and breeding programs, as well as for studying carbohydrate metabolism during ripeness and postharvest storage (Guan et al., 2015). For industrial purposes, breeding and research there is a strong need for rapid and non-destructive determination of SSC as well as the individual sugars in apples.

Near-infrared spectroscopy (NIRS) is already established as an efficient method for determination of SSC in apples. The method relies on absorption overtones and combination of vibrational bands mainly associated with -CH and -OH functional groups present in the different carbohydrates such as glucose, sucrose and fructose (López et al., 2016). Nicolaï et al., 2007 reviewed the status of non-destructive measurement of fruit quality by means of NIRS, and several studies show that a typical prediction error (root mean square error of prediction, RMSEP) for SSC is around 0.5 %. But this accuracy is usually obtained for individual apple varieties from the same season and from the same orchard. When calibrations are validated with apples from different seasons or origins, the RMSEP usually increases to 1-1.5 %. Nicolaï et al., 2007 concluded that to obtain a robust calibration model, the calibration data set should be rich in variation and include apples from different orchards and seasons. They regarded model robustness as the single most important concern in NIRS of horticultural produce. The use of NIRS for determination of individual sugars

63   in intact apples was newly reported by Lan et al. (2020). They collected spectra in the region 900-

64   2500 nm from 840 apples of three varieties. Calibration models for fructose, glucose and sucrose

65   were obtained with promising results (RMSEP = 1.9, 9.2 and 7.6 g/kg, respectively). The models

66   were complex and no interpretation of the spectral data was offered (Lan et al., 2020).

67   Today, grading lines equipped with NIR sensors are commercially available (Nicolaï et al., 2007)

68   and novel compact sensors have the potential to be used effectively in field and during storage.

69   But the workload of proper calibration and continuous calibration maintenance is a considerable

70   cost. It is therefore of interest to explore potential alternative non-destructive techniques. Raman

71   spectroscopy is one such technique that is now available in more affordable and compact

72   instrumentation. Raman spectra are in general more selective compared to NIR spectra, providing

73   more narrow spectral bands with abundant and well resolved chemical information which is easier

74   to interpret. It is well known that Raman spectroscopy is well suited for analysis and

75   quantification of sugars in complex samples. Özbalci et al., 2013 showed that fructose, glucose,

76   maltose and sucrose in water solutions can be clearly discriminated, and also quantified in diluted

77   honey samples by Raman spectroscopy using a laser excitation of 785 nm. Calibration models

78   based on PLS regression gave correlation coefficients higher than 0.95 for all the individual

79   sugars (Özbalci et al., 2013). Individual sugars in soft drinks have also been quantified with

80   Raman, using external calibration curves with sugar standards (Ilaslan et al., 2015). In this case,

81   Raman spectroscopy performed equally well as high performance liquid chromatography. Raman

82   spectroscopy is suitable for process monitoring in liquid systems and has been used for real time

83   quantification of total sugars with high accuracy (R^2 = 0.99, RMSECV = 0.17 g/L) during wine

84   fermentation (Wang et al., 2014). Total sugars were also determined in wine samples by FT-

85   Raman (RMSEP = 0.85 g/L) and better results were obtained compared to mid IR (RMSEP = 1.2

86   g/L) and NIRS (RMSEP = 1.4 g/L). Raman spectroscopy has also been used for adulteration

87   detection of coconut water with different types of sugars and was demonstrated to detect very low

88   levels of added single sugars, i.e. 2.1 %, 2.6 % and 1.9 % for glucose, fructose and sucrose,

89   respectively (Richardson et al., 2019).

One important technical aspect when considering Raman spectroscopy for analysis of intact solid food matrices is representative sampling. Novel Raman system designs, such as spatially offset Raman spectroscopy (SORS) and wide area Raman spectroscopy, allow deeper optical sampling in biological tissues (Esmonde-White et al., 2017; Monago-Maraña et al., 2021). This makes them highly relevant for measuring internal quality in foods (Afseth et al., 2014). An example is the use of SORS for evaluation of internal maturity of tomatoes (Qin et al., 2012). As far as we know, there are no reported studies on the determination of SSC or individual sugars in intact apples by Raman spectroscopy. Hence, the aim of this study was to elucidate the potential for such an application. Raman measurements employing a wide area Raman probe were performed on a total of 60 apples of six different varieties at three steps: 1. intact apples, 2. apples without skin, and 3. on the juice from the apples. From these measurements, regression models for SSC (%), total sugars and contents of sucrose, glucose and fructose were obtained. In addition, the optical sampling depth in apples was investigated.

2. Materials and methods

2.1. Samples and chemicals

A total of 60 samples were used in this study. Ten apples of six different varieties were selected from the Norwegian grocery market in 2020: Granny Smith (variety 1), Royal Gala Kanzi (variety 2), Royal Gala (variety 3), Golden Delicious (variety 4), Pink Lady (variety 5) and Ecology Red apples (variety 6). All samples were purchased May 2020 and could thus be expected to be fully ripened. They were kept at 4 ºC until further analysis.

Glucose, fructose and sucrose standards were purchased from Merck (Oslo, Norway). Trehalose was obtained from VWR Life Science (Oslo, Norway). Sodium acetate and sodium hydroxide solution (50 – 52 % in water), used for the mobile phases, were bought from Merck (Oslo, Norway). Milli-Q water was obtained from a Milli-Q water system (Merck, Oslo, Norway).

2.2. Reference analysis

Soluble solids content (SSC), expressed in %, was determined at 25 ºC with a RE40 digital refractometer (Mettler Toledo AS, Oslo) on the fresh juice samples obtained, from peeled apples after removing the peduncle, with a juice maker. Juices were then frozen for further analysis of glucose, fructose and sucrose. Individual sugars were determined following the method described by Helgerud et al., 2016. An aliquot of juice was diluted (1:2000) with Milli-Q water and containing 10 μg/mL of trehalose as internal standard in each sample. A High-Performance Anion Exchange Chromatography with Pulse Amperometric Detection (HPAED-PAD) system was employed (Dionex ICS 5000+, Thermo Scientific Inc., USA). The system was equipped with an AS-AP autosampler, an ICS 5000+SP pump and an ICS 5000+DC column oven. An ICS 5000+ED pulsed amperometric detector, with an Au working electrode and an Ag/AgCl reference electrode was used. A CarboPac PA-1 anion exchange column and a CarboPac PA-1 guard column were used and kept at 25 ºC. Elution was performed in isocratic mode with sodium hydroxide (100 mM) for 15 min, followed by a washing step for 5 min with sodium hydroxide (100 mM) in sodium acetate (500 mM). The column was then reconditioned for 5 min with sodium hydroxide (100 mM) before next injection. Flow rate was set at 1 mL/min and an injection volume of 20 μL was employed. All samples were analyzed in duplicate.

2.3. Raman spectroscopy

A RamanRXN2^{TM} Hybrid system (Kaiser Optical Systems, Inc., Ann Arbor, MI, USA) was used to collect the Raman spectra. This instrument was equipped with a wide area non-contact PhAT-probe. A 400 mW laser with a 785 nm excitation wavelength, and a circular spot size of D = 6 mm at a 25 cm working distance was used. Each spectrum was an average of 4x20 sec accumulations, measured in triplicate, giving a total acquisition time of 320 seconds for each sample. The average of the three spectra were taken after fluorescence background correction. The measured spectral range was 200 – 1890 cm^{-1}. All samples were measured during four days in a random sequence to avoid potential systematic variations between days or varieties.

142 To account for possible heterogeneity of samples, apples were spinned around their own axis

143 during spectral collection. Each sample was first measured with skin. The apples were then peeled

144 with a vegetable peeler and measured again. Finally, juice from each apple was obtained with a

145 juice maker (Philips HR1866/00). The peduncle was removed and the remaining of peeled apple

146 was juiced. The juices were frozen after measuring SSC for further analysis with a different

147 Raman probe. The time for the entire procedure was less than 20 minutes per apple, avoiding

148 oxidation of samples with air.

149 All juice samples were thawed and measured with a Raman immersion ballprobe (Matrix

150 Solutions, Bothell, WA) suitable for liquids. The ballprobe was 20 cm long and 12.5 mm o.d,

151 incorporating a spherical lens. The instrumental settings were the same as those used for solid

152 samples, again performed in triplicates.

153

154 **2.4. Depth of Raman measurement**

155 To investigate the sampling depth with Raman in intact apples we performed one simple

156 experiment. A 25 mm thick slice of apple was placed upon a slice of carrot. The skin side of the

157 apple was facing the Raman probe (Figure 1). The apple slice was gradually sliced thinner and

158 thinner from the underside, and for every thickness a Raman spectrum was recorded. The thinnest

159 slice was 2 mm thick. The experiment was done for two apple slices, one without skin and one

160 with red skin. The appearance of the beta-carotene peaks at the different sample thicknesses

161 would give an indication of the sampling depth. Multivariate curve resolution (MCR) was used

162 to extract the pure carrot and apple signals from the spectra (Tauler, 1995), making it possible to

163 estimate the relative contributions from carrot and apple as function of apple slice thickness. MCR

164 was performed in Matlab version R2007b by the PLS_Toolbox (Eigenvector Research Inc.,

165 Manson, WA, USA).

166

167

2.5. Multivariate data analysis

The fluorescence background in the raw Raman spectra was removed by subtracting a polynomial fitted to the baseline (Lieber and Mahadevan-Jansen, 2003). The procedure was applied to the range 300 - 1500 cm^{-1} because the main information from sugars is in this range. A polynomial degree of 6 was used. The correction was performed using in-house Matlab scripts (R2007b, The MathWorks, Inc., Natick, MA, USA).

Principal component analysis (PCA) (Wold et al., 1987) was applied to explore spectral variation between apple varieties. PCA was performed using The Unscrambler version 6.11 (CAMO Software AS, Oslo, Norway). Partial least-squares regression (PLSR) (Martens and Næs, 1989) was used to obtain calibration models between Raman spectra and the quality features. Full cross-validation and segmented cross-validation (leaving out one apple variety at the time) were used to determine the number of components to use in the calibrations, and to evaluate the performance of the models. Multivariate calibration was performed using The Unscrambler version 6.11 (CAMO Software AS, Oslo, Norway).

3. Results and discussion

3.1. Spectral information

Baseline corrected Raman spectra of apples with and without skin, as well as for apple juice, are presented in Figure 2 (raw spectra are shown in Figure S1). The spectra clearly reveal that Raman spectra of apples are rich in bands and thus chemical information on apple composition. Tentative band assignments are provided in Table 1, and as seen from the list, most bands can be attributed to the carbohydrates sucrose, fructose and glucose (Ilaslan et al., 2015; Özbalci et al., 2013). The most intense bands appear at 629 cm^{-1} and 1459 cm^{-1}. Raman spectra of glucose, fructose and sucrose standards collected in water solution are provided in Figure S2. By comparing the spectra, a range of the bands appearing in apple spectra can be identified in the standards: 420 cm^{-1}

193 (fructose or glucose); 629 cm^{-1} (fructose), 1084 cm^{-1} (fructose), 1124 cm^{-1} (glucose), 1264 cm^{-1}

194 (fructose) and 1459 cm^{-1} (fructose, sucrose or glucose).

195 Figure 2 reveals notable similarity between apple juice spectra and spectra of apples without skin.

196 More surprising, taking into account the colorful skin, Raman spectra of apples with and without

197 skin are also very similar. This similarity could be related to the fact that apple skin is rather thin

198 and that we were probing considerably deeper into the apple. The few additional bands found in

199 the spectra of apples with skin is most likely related to skin pigmentation, such as chlorophyll

200 (i.e. the Raman bands found at 746 cm^{-1} and 1327 cm^{-1}) (Jehlička et al., 2014). All spectra in

201 Figure 2 are colored according to SSC (%) values. By visual inspection, a clear trend in the spectra

202 is observed in some regions around 629, 854, 1084, 1124, 1264 and 1459 cm^{-1}. These bands are

203 more intense in samples of high SSC. The trend is more apparent for apples without skin and

204 juices compared with spectra from samples with skin and thus gives initial indications on the

205 quantitative features of the spectra.

206 To study potential spectral variation among apple varieties, detect potential outliers and

207 systematic artifacts in the samples, PCA was applied. For apples with skin, the second and fourth

208 principal components (PC2 and PC4)), explaining 23 % and 4 % of the variance, respectively,

209 showed a quite clear clustering of samples according to varieties (Figure 3A). Loadings for PC2

210 (Figure 3B) show that the main variables affecting the separation of varieties were 628, 835, 1083

211 and 1458 cm^{-1}, representing bands from sucrose and fructose. Scores values for PC2 were

212 generally higher for varieties 2, 3, 5 and 6, which indicates that the concentrations of these

213 compounds tend to be higher in these varieties. This is in accordance with measured sucrose

214 (Figure 5). For PC4, the variables resulting in clustering were 420, 628, 745 and 1326 cm^{-1}.

215 Positive loadings were related with glucose and fructose and negative loadings were related with

216 chlorophyll, showing higher intensity peaks in variety 1, 3 and 5 for these variables.

217 In the case of apples without skin, PC2 and PC3, explaining 22 and 7 % of variance, respectively,

218 showed some clustering (Figure 3C). Variety 5 was the most clearly clustered group. For PC3,

219 the main variables highlighted were 628, 834, 1124 and 1456 cm^{-1}. Positive loadings (1124 cm^{-1})

220 were related with glucose, which was very low for variety 5 (Figure 5C). Negative loadings were

221 related with sucrose and fructose, and the concentration of sucrose was high in variety 5.   Thus,

222 even though apple skin clearly introduces additional chemical information in the spectra, clear

223 chemical features from apple tissue is seen in both sampling approaches.

224

225 **3.2. Depth of Raman measurement**

226 A simple experiment was performed to investigate Raman sampling depth in intact apples using

227 a thick slice of apple on top of a slice of carrot. The carrot exhibits strong Raman scattering at

228 1007 cm^{-1} and 1156 cm^{-1} due to beta-carotene. Figure 4A shows Raman spectra from the apple

229 slices of varying thickness upon the carrot sample. The intensity of the beta-carotene bands

230 increased when the thickness of the apple slices decreased. Based on MCR it was possible to

231 separate the signals from carrot and apple, and the estimated pure spectra are shown in Figure 4B.

232 The corresponding estimated concentrations of carrot and apple for each apple slice thickness are

233 plotted in Figure 4C and 4D. The estimated concentrations were normalized with respect to the

234 signals obtained from pure carrot and apple, respectively, and are therefore estimates of how large

235 shares of the signal that originated from carrot or apple. For an apple slice of 2 mm without skin

236 (Figure 4C) about 55 % of the signal came from the carrot, and for a slice of 5 mm as much as 27

237 % of the signal still came from carrot. At 8 mm thickness the contribution from carrot was

238 approaching zero. For apple with skin the signal contribution from deeper regions was smaller,

239 about 30 % at 2 mm and 12 % at 5 mm thickness. It was concluded that the current setup was

240 sufficient to probe 7-8 mm into the apple and that the skin reduced the signal from deeper regions.

241 Clearly, most of the Raman signal came from the sample volume close to the apple surface (0-4

242 mm), but it is interesting that signals are captured from depths down to 8 mm. Similar studies

243 with NIR spectroscopy on apples indicate a sampling depth of only about 4 mm in the 700–900

244 nm range (Lammertyn et al., 2000), but sampling depth will always depend on the optical setup.

245

3.3. Quantification of SSC and sugars

The bar charts of Figure 5 show the variation of all the analyzed reference parameters, grouped by variety. For SSC there are similar ranges (minimum and maximum values) across all varieties (Figure 5A). Samples from variety 1 (Granny Smith) and variety 4 (Golden Delicious) had lower total content of sugars than the other four varieties (Figure 5B). Larger span of variation (both between varieties and within each variety) is seen for glucose (Figure 5C) and sucrose (Figure 5E) compared to fructose (Figure 5D). Mean values of fructose for each variety were compared, and statistically differences were found between varieties 6 and 1 and varieties 6 and 5. The correlations found between different reference parameters in the samples were calculated and are provided in Figure S3A. As expected, there was a high correlation between SSC (%) and total sugars. In addition, there were high and positive correlations between sucrose, SSC and total sugars. A strong negative correlation was found between sucrose and glucose. Fructose did not present high correlations towards any other parameter. In general, these correlations are important to take into account when interpreting the calibration models obtained.

Baseline corrected Raman spectra ($300 - 1500$ cm^{-1}) were used to obtain the calibration models for all chemical reference parameters (Table 2). The optimal number of components were chosen based on the explained variance for each component as well as the regression coefficients, making sure regression coefficients were consisting of distinct spectral features and not only noise. For SCC, the results were good compared to reported studies based on NIRS (Fan et al., 2020; Lan et al., 2020; Li et al., 2018). In general, results based on apples without skin were better than apples with skin. This result could be expected since having to penetrate the skin adds complexity to the spectroscopic measurements. Moreover, reference measurements were obtained from the peeled apples, so a better match could be expected. However, results for the measurements on apples with skin are still acceptable. Regression coefficients for all calibration models for apples without skin are provided in Figure 6. For the SSC regression coefficients (Figure 6A), the main variables affecting the models were found at 834, 1070, 1130 and 1460 cm^{-1}. These variables have been attributed to sucrose in solution (Figure S2C). This result is in accordance with the correlation

273 found between SSC and sucrose content (Figure S3). Overall, the regression coefficients for total

274 sugars emphasized similar chemical bands as those for SSC.

275 For glucose and sucrose, good calibration models were obtained, both on apples with and without

276 skin. The regression coefficients for glucose and sucrose were dominated by the same Raman

277 bands, but inversely correlated. This could be expected since the reference values were negatively

278 correlated (Figure S3A). The correlations between the predicted values from these calibration

279 models are shown in supplementary Figure S3B and S3C. Since these correlation coefficients

280 were similar to those obtained for the reference values, it is most likely possible to predict the

281 individual content of sugars independently of the variation of other sugars or total sugars. The

282 poorest regression results were obtained for fructose for all sample types. However, note that the

283 regression coefficients obtained (Figure 6D) (including the following Raman shifts: 423, 523,

284 629, 1268 and 1460 cm^{-1}) closely resembles the Raman spectrum of aqueous fructose (Figure

285 S2B and Table 1). This means that the model is based on chemical information from fructose.

286 One explanation for poor accuracy is the narrow variation range of fructose, as seen in Figure 5D.

287 Calibration models for juice were included as benchmarks for the other sampling approaches,

288 since juice samples are more homogeneous without the complex sample matrix of intact apples.

289 Surprisingly, for SCC and total sugars, regression results were better for apples without skin than

290 for juice samples. For single sugars, the regression results obtained on apples without skin were

291 very similar to those of juice. It is difficult to point on one single explanation for these results.

292 For bulk parameters like SCC and total sugars it could be hypothesized that apple matrix bands

293 not directly related to sugars are used indirectly to improve modelling of bulk parameters in the

294 peeled apples. Such matrix bands are obviously not present in juice spectra. Regardless, the results

295 clearly suggest that apple measurements perform as well as juice measurements, which is

296 encouraging for future development of this application.

297 In this study, all Raman spectra were pre-processed using a standard baseline correction.

298 Additional tests employing a normalization routine (extended multiplicative scattering correction)

299 led to less accurate calibration models (data not shown). Normalization could remove relevant

chemical variation in the Raman spectra. The exploration of pre-processing steps, including baseline correction and normalization, will be an essential part of future development of this approach. Moreover, in order to evaluate the robustness of the Raman measurements, regression models were validated by leaving out one apple *variety* at a time (i.e. 17 % of the samples were left out each time). As provided in Table S1, these results were mainly the same as for full cross-validation. Since robustness across varieties is a major challenge when using NIR spectroscopy, this suggests that Raman could be a beneficial alternative. However, more data is needed to explore this possibility.

To validate current results, sample sets and variation ranges should be extended with new varieties. As only ripe apples with very low starch contents were used, the inclusion of apples from different stages of ripening would also be very interesting. Starch exhibits distinct Raman bands that certainly will affect the overall Raman fingerprints. Another interesting aspect is looking into alternative Raman sampling possibilities. SORS could potentially provide deeper optical sampling than the wide area Raman probe used in the present study, and this might improve current results. SORS is expected to be particularly beneficial in measurements of intact apples, since the SORS approach would enable efficient penetration and suppression of signals from the skin layer.

Compared to NIRS, Raman systems are generally limited by weaker signals. Prolonged exposure times is a common way of compensating for this. The exposure times used in the current study (i.e. 320 seconds) were not optimized with respect to speed, but an achievable aim should be to reduce exposure times down to 2-5 seconds. Furthermore, Raman measurements are very sensitive to ambient light. In this study the measurements were done in a dark room with negligible ambient light, while in field or in processes this has to be solved with proper shielding. In addition, Raman systems tend to be more expensive than NIR systems. The development of Raman technology is currently happening at a steady pace, and it is likely that more affordable systems with improved sampling opportunities and signal efficiency will be available in the near future.

4. Conclusions

This study illustrates the feasibility of using Raman spectroscopy for quantification of SSC and individual sugars (glucose, fructose and sucrose) in apples with and without skin. By using a wide area Raman probe, it is possible to measure at least 8 mm into an apple, through the skin. Calibration models for SSC provided an accuracy comparable with what is achievable with NIRS. In addition, good calibration models were obtained for glucose and sucrose. Poorest models were obtained for fructose. This could be related to the poor variation range of this component in the current sample set. Extending sample sets with new varieties at different stages of ripeness is needed to further validate the feasibility of Raman spectroscopy for use in apple quality evaluation.

345   **References**

346   Afseth, N.K., Bloomfield, M., Wold, J.P., Matousek, P., 2014. A novel approach for subsurface through-

347   skin analysis of salmon using spatially offset raman spectroscopy (sors). Appl. Spectrosc. 68, 255–

348   262. https://doi.org/10.1366/13-07215

349   Cael, J.J., Koenig, J.L., Blackwell, J., 1974. Infrared and raman spectroscopy of carbohydrates.

350   Carbohydr. Res. 32, 79–91. https://doi.org/10.1016/s0008-6215(00)82465-9

351   Delfino, I., Camerlingo, C., Portaccio, M., Ventura, B. Della, Mita, L., Mita, D.G., Lepore, M., 2011.

352   Visible micro-Raman spectroscopy for determining glucose content in beverage industry. Food

353   Chem. 127, 735–742. https://doi.org/10.1016/j.foodchem.2011.01.007

354   Esmonde-White, K.A., Cuellar, M., Uerpmann, C., Lenain, B., Lewis, I.R., 2017. Raman spectroscopy

355   as a process analytical technology for pharmaceutical manufacturing and bioprocessing. Anal.

356   Bioanal. Chem. 409, 637–649. https://doi.org/10.1007/s00216-016-9824-1

357   Fan, S., Wang, Q., Tian, X., Yang, G., Xia, Y., Li, J., Huang, W., 2020. Non-destructive evaluation of

358   soluble solids content of apples using a developed portable Vis/NIR device. Biosyst. Eng. 193,

359   138–148. https://doi.org/10.1016/j.biosystemseng.2020.02.017

360   Guan, Y., Peace, C., Rudell, D., Verma, S., Evans, K., 2015. QTLs detected for individual sugars and

361   soluble solids content in apple. Mol. Breed. 35, 1–13. https://doi.org/10.1007/s11032-015-0334-1

362   Harker, F.R., Gunson, F.A., Jaeger, S.R., 2003. The case for fruit quality: An interpretive review of

363   consumer attitudes, and preferences for apples. Postharvest Biol. Technol. 28, 333–347.

364   Helgerud, T., Knutsen, S.H., Afseth, N.K., Stene, K.F., Rukke, E.O., Ballance, S., 2016. Evaluation of

365   Hand-Held Instruments for Representative Determination of Glucose in Potatoes. Potato Res. 59,

366   99–112. https://doi.org/10.1007/s11540-015-9310-8

367   Ilaslan, K., Boyaci, I.H., Topcu, A., 2015. Rapid analysis of glucose, fructose and sucrose contents of

368   commercial soft drinks using Raman spectroscopy. Food Control 48, 56–61.

369   https://doi.org/10.1016/j.foodcont.2014.01.001

370 Janick, J., Cummins, J.N., Brown, S.K., Hemmat, M., 1996. Apples, in: Janick, J., Moore, J.N. (Eds.),
371   Fruit Breeding: Volume I. Tree and Tropical Fruits. Wiley, New Jersey, pp. 1–77.

372 Jehlička, J., Edwards, H.G.M., Oren, A., 2014. Raman spectroscopy of microbial pigments. Appl.
373   Environ. Microbiol. 80, 3286–3295. https://doi.org/10.1128/AEM.00699-14

374 Lammertyn, J., Peirs, A., De Baerdemaeker, J., Nicolaï, B., 2000. Light penetration properties of NIR
375   radiation in fruit with respect to non-destructive quality assessment. Postharvest Biol. Technol. 18,
376   121–132. https://doi.org/10.1016/S0925-5214(99)00071-X

377 Lan, W., Jaillais, B., Leca, A., Renard, C.M.G.C., Bureau, S., 2020. A new application of NIR
378   spectroscopy to describe and predict purees quality from the non-destructive apple measurements.
379   Food Chem. 310, 125944. https://doi.org/10.1016/j.foodchem.2019.125944

380 Li, X., Huang, J., Xiong, Y., Zhou, J., Tan, X., Zhang, B., 2018. Determination of soluble solid content
381   in multi-origin 'Fuji' apples by using FT-NIR spectroscopy and an origin discriminant strategy.
382   Comput. Electron. Agric. 155, 23–31. https://doi.org/10.1016/j.compag.2018.10.003

383 Lieber, C.A., Mahadevan-Jansen, A., 2003. Automated method for subtraction of fluorescence from
384   biological Raman spectra. Appl. Spectrosc. 57, 1363–1367.

385 López, M.G., García-González, A.S., Franco-Robles, E., 2016. Carbohydrate analysis by NIRS-
386   Chemometrics. Intech 13.

387 Martens, H., Naes, T., 1989. Multivariate Calibration. Wiley, New York.

388 Monago-Maraña, O., Wold, J.P., Rødbotten, R., Dankel, K.R., Afseth, N.K., 2021. Raman, near-infrared
389   and fluorescence spectroscopy for determination of collagen content in ground meat and poultry
390   by-products. Lwt 140. https://doi.org/10.1016/j.lwt.2020.110592

391 Nicolaï, B.M., Beullens, K., Bobelyn, E., Peirs, A., Saeys, W., Theron, K.I., Lammertyn, J., 2007.
392   Nondestructive measurement of fruit and vegetable quality by means of NIR spectroscopy: A
393   review. Postharvest Biol. Technol. 46, 99–118.

394 Özbalci, B., Boyaci, I.H., Topcu, A., Kadilar, C., Tamer, U., 2013. Rapid analysis of sugars in honey

395   by processing Raman spectrum using chemometric methods and artificial neural networks. Food

396   Chem. 136, 1444–1452. https://doi.org/10.1016/j.foodchem.2012.09.064

397   Qin, J., Chao, K., Kim, M.S., 2012. Nondestructive evaluation of internal maturity of tomatoes using

398   spatially offset Raman spectroscopy. Postharvest Biol. Technol. 71, 21–31.

399   https://doi.org/10.1016/j.postharvbio.2012.04.008

400   Richardson, P.I.C., Muhamadali, H., Ellis, D.I., Goodacre, R., 2019. Rapid quantification of the

401   adulteration of fresh coconut water by dilution and sugars using Raman spectroscopy and

402   chemometrics. Food Chem. 272, 157–164. https://doi.org/10.1016/j.foodchem.2018.08.038

403   Söderholm, S., Roos, Y.H., Meinander, N., Hotokka, M., 1999. Raman spectra of fructose and glucose

404   in the amorphous and crystalline states. J. Raman Spectrosc. 30, 1009–1018.

405   https://doi.org/10.1002/(sici)1097-4555(199911)30:11<1009::aid-jrs436>3.0.co;2-%23

406   Tauler, R., 1995. Multivariate curve resolution applied to second order data. Chemom. Intell. Lab. Syst.

407   30, 133–146. https://doi.org/10.1016/0169-7439(95)00047-X

408   Wang, Q., Li, Z., Ma, Z., Liang, L., 2014. Real time monitoring of multiple components in wine

409   fermentation using an on-line auto-calibration Raman spectroscopy. Sensors Actuators, B Chem.

410   202, 426–432. https://doi.org/10.1016/j.snb.2014.05.109

411   Wold, S., Esbensen, K.I.M., Geladi, P., 1987. Principal Component Analysis. Chemom. Intell. Lab.

412   Syst. 2, 37–52.

413

Table 1. Tentative assignment of Raman bands found in apple samples.				
Wavenumber (this work) (cm^{-1})	Wavenumber reference (cm^{-1})	Vibration	Compound assigned	Reference
420	415	δ(C2 - C1-O1)	Glucose	(Ilaslan et al., 2015)
	419	δ(C - C-O)	Fructose	(Özbalci et al., 2013)
519	523	Skeletal vibration	Glucose	(Ilaslan et al., 2015)
629	631	δ(C–C–O)	Fructose	(Ilaslan et al., 2015)
802	800	ν(C-C)	Sucrose	(Ilaslan et al., 2015)
854	856	δ(C1 – H1)	β-glucose	(Özbalci et al., 2013)
1084	1082	ν(C-O)	Fructose	(Söderholm et al., 1999)
1124	1127	-	β-glucose	(Cael et al., 1974)
1264	1263	-	β-glucose	(Cael et al., 1974)
	1264		Fructose	(Delfino et al., 2011)
1459	1459	-CH$_2$	Fructose	(Delfino et al., 2011)
	1460		Glucose	(Söderholm et al., 1999)

414

		Apples with skin	Apples without skin	Juices
Table 2. Results obtained for the different models.				
SSC	**Comp.**	2	1	4
	RMSECV (%)	0.66	0.46	0.72
	R²	0.70	0.85	0.63
Total sugars	**Comp.**	2	2	2
	RMSECV (mg/L)	9.7	7.5	9.3
	R²	0.57	0.74	0.61
Glucose	**Comp.**	6	3	3
	RMSECV (mg/L)	2.8	1.9	2.1
	R²	0.82	0.91	0.90
Fructose	**Comp.**	3	4	3
	RMSECV (mg/L)	6.2	5.6	6.0
	R²	0.27	0.40	0.32
Sucrose	**Comp.**	5	3	2
	RMSECV (mg/L)	5.8	3.9	3.6
	R²	0.89	0.95	0.96

415

		Apples with skin	Apples without skin	Juices

Figure captions

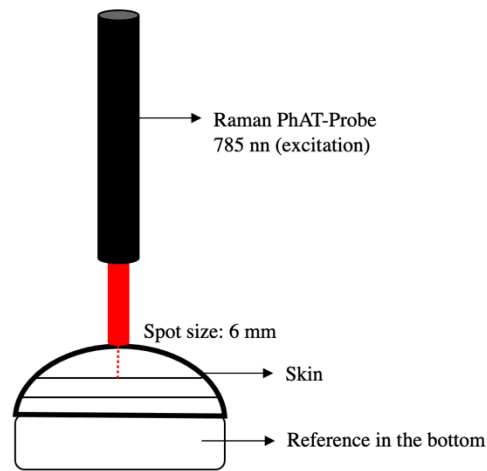**Figure 1.** Sketch of sampling approach for the depth measurement study.

Figure 2. Baseline-corrected Raman spectra from apples with skin (A), apples without skin (B) and apple juices (C). Spectra are colored according to SSC.

Figure 3. Scores values (A and C) and loadings (B and D) obtained from PCA analysis of apples with skin (A and B) and without skin (C and D).

Figure 4. Baseline-corrected Raman spectra obtained for the different slices of apples without skin (A). Estimated pure spectra obtained by MCR (B). Estimated concentrations by MCR for apple without skin (C) and with skin (D).

Figure 5. Bar charts for the different parameters studied: SSC (A), total sugars (B), glucose (C), fructose (D) and sucrose (E). Light colors represent the minimum values, dark colors represent the maximum values and medium color represents the mean value. The error bars represent the standard deviation in each case.

Figure 6. Regression coefficients for the models obtained for apples without skin: SSC (A), total sugars (B), glucose (C), fructose (D) and sucrose (E).
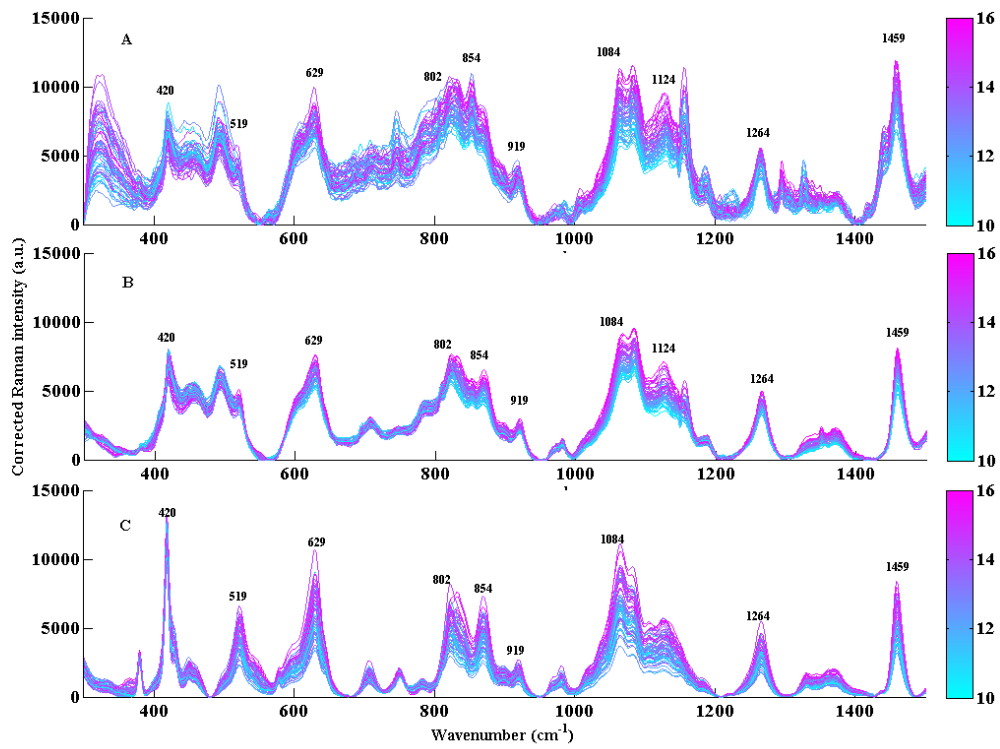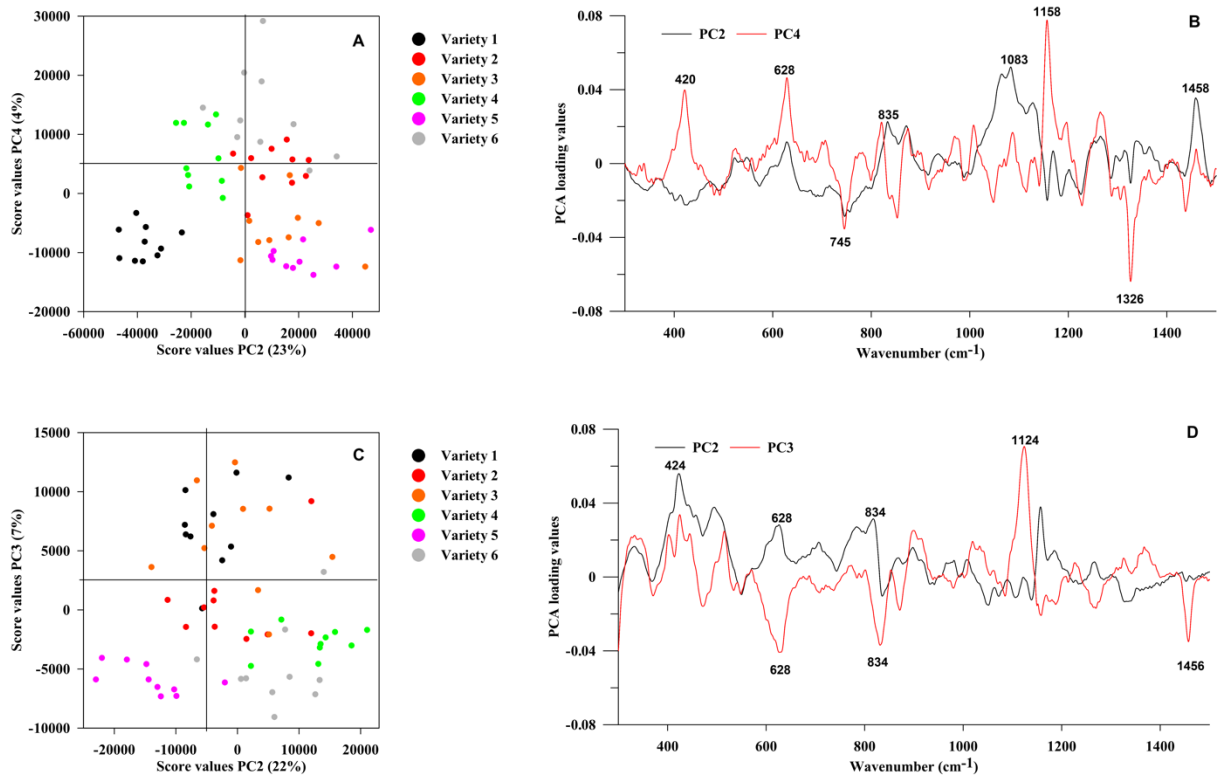
431

432   **Figure 1**

433

434

435

436   **Figure 2**

437

438

439

440   **Figure 3**

441

442

443   **Figure 4**

444

445

446

447

448

Figure 5
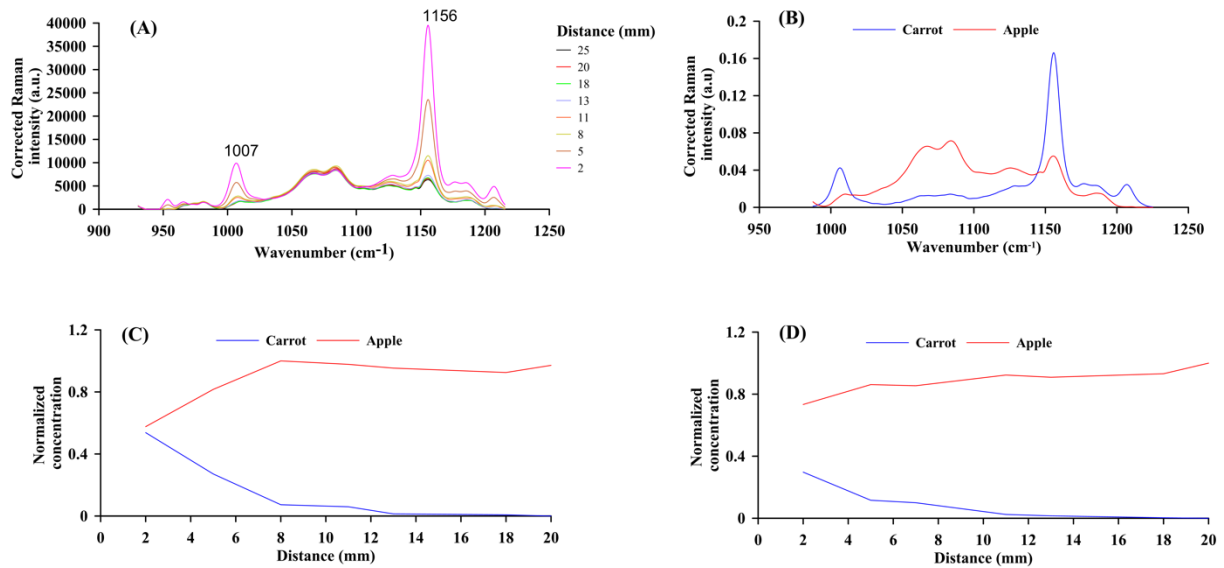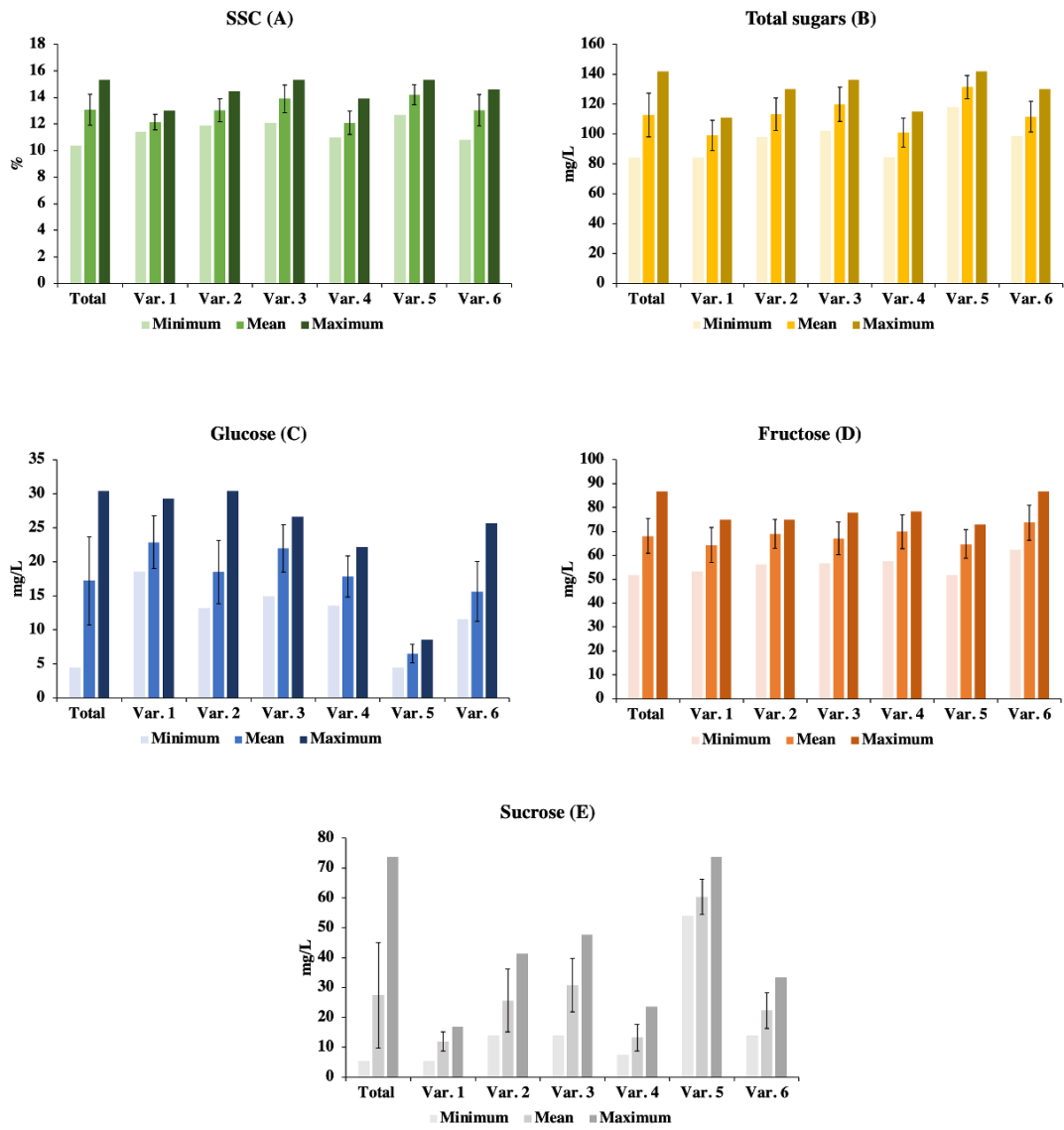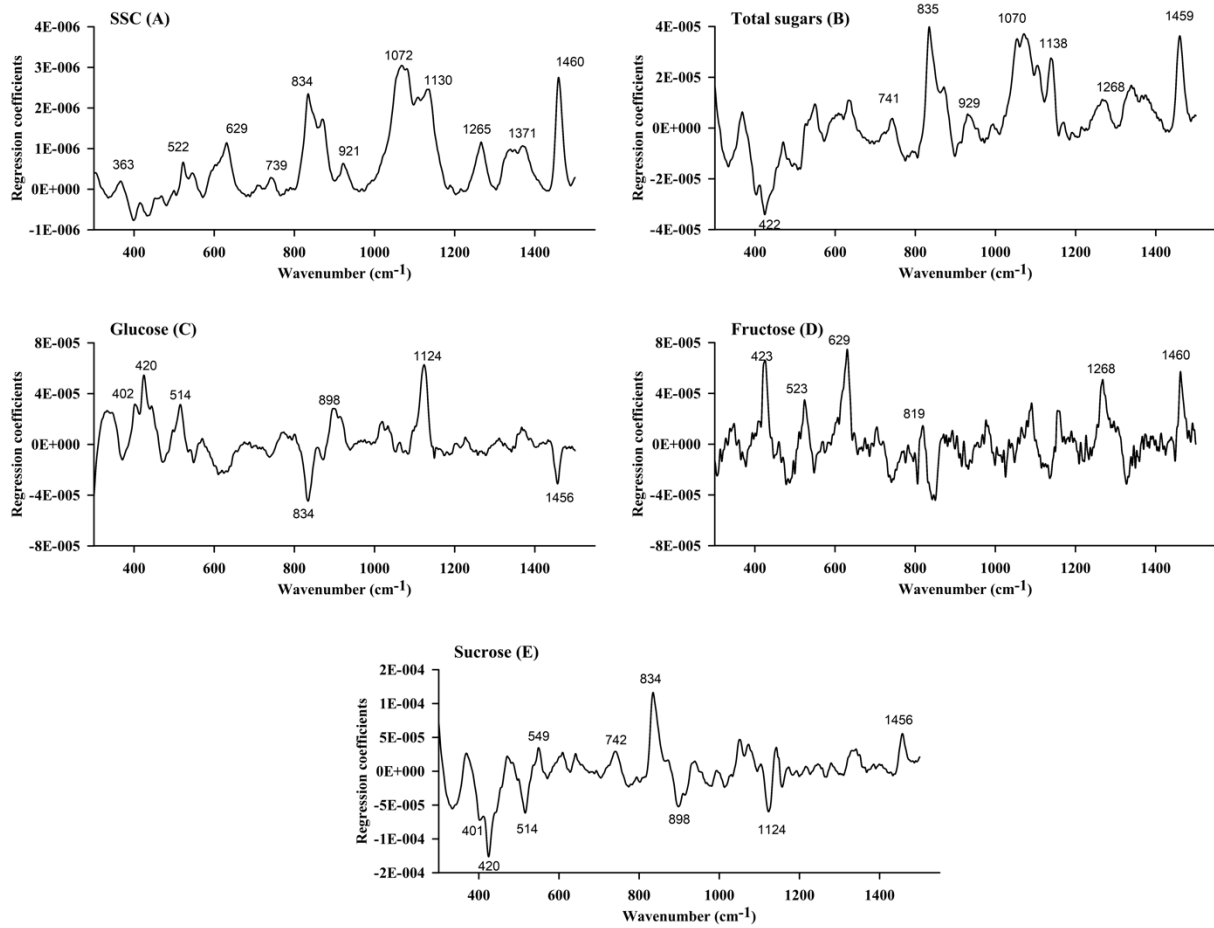
449

450

451

452

453

454

455

456   **Figure 6**